NASA
Technical
Paper
1999

May 1982

Computer Modeling of Multiple-Channel Input Signals and Intermodulation Losses Caused by Nonlinear Traveling-Wave-Tube Amplifiers

N. Stankiewicz

NASA

NASA
Technical
Paper
1999

1982

Computer Modeling of Multiple-Channel Input Signals and Intermodulation Losses Caused by Nonlinear Traveling-Wave-Tube Amplifiers

N. Stankiewicz
Lewis Research Center
Cleveland, Ohio

NASA
National Aeronautics
and Space Administration

**Scientific and Technical
Information Branch**

Summary

The multiple-channel input signal to a soft limiter amplifier such as a traveling wave tube is represented as a finite, linear sum of Gaussian functions in the frequency domain. Linear regression is used to fit the channel shapes to a least-squares residual error.

Distortions in output signal, namely intermodulation products, are produced by the nonlinear gain characteristic of the amplifier and constitute the principle noise analyzed in this study. The signal-to-noise ratios are calculated for various input powers from saturation to 10 dB below saturation for two specific distributions of channels.

A criterion for the truncation of the series expansion of the nonlinear transfer characteristic is given. It is found that the signal-to-noise ratios are very sensitive to the coefficients used in this expansion. Improper or incorrect truncation of the series leads to ambiguous results in the signal-to-noise ratios.

Introduction

The multichannel use of an amplifier in a communications system requires linear operation in order to prevent interference between channels. For a soft-limiting, nonlinear device such as a traveling wave tube (TWT) amplifier this means backing off below saturation to the linear portion of the gain curve. Such quasi-linear operation results in an unavoidable loss of efficiency which can be partially recovered in a TWT through the use of a depressed collector.

Despite the advances (ref. 1) of multistaged depressed collectors in recovering the spent beam energy of TWT's, it is important to determine the extent of the backoff if the highest possible efficiency is to be achieved. This importance manifests itself in two ways. First, the collector design is a function of the TWT operating point. And second, the TWT gain characteristics may be a design option to be traded with other parameters; for example, the length of the slow wave structure.

The principal nonlinearity of TWT's affecting efficiency is the power gain characteristic (AM/AM conversion). This type of nonlinearity wastes power directly by producing intermodulation bands and by broadening the channel signals. These out-of-band signals must be removed with filters and represent a loss in available power.

Other nonlinearities such as amplitude-to-phase conversion (AM/PM) also affect efficiency but indirectly through distortion of the input signal. Acceptable signal quality depends upon the type of modulation and demodulation to be used. Such considerations are beyond the scope of this paper. It will be assumed that operating quasi-linearly to diminish AM/AM conversion will also diminish AM/PM distortions to an acceptable level. Therefore, only the AM/AM characteristics will be discussed in this report.

The purpose of the work reported in this paper is to develop a computational program to evaluate AM/AM channel interference in a TWT. The computer program is designed to use empirical data in the modeling of the input channel spectra and also for the gain characteristics.

By channel spectra we mean the amplitude distribution of the channels as a function of frequency. Early in the development of this computer program it was decided that modeling of input spectrum was a desirable option for several reasons. First, this approach provides flexibility in analyzing input signals without direct consideration of the method of modulation or signal coding that may be used in the communications system. Second, questions concerning accurate representations of signals which convey real information and which are usually handled by taking ensemble averages (ref. 2) over these randomly occurring variables can be circumvented. Finally, the method chosen for the modeling of the channels, a least-squares expansion in Gaussian functions, is reminiscent of the central limit theorem in which the cumulative effect of many random processes tends to a Gaussian distribution.

It was envisioned that this work would be supplemented by an auxiliary systems program which would simulate a modulation technique, perform an ensemble average over a random signal (both information as well as noise) and spectrally analyze the result. This or, perhaps, measured spectral data would be the input for the AM/AM interference program.

The voltage gain curve must also be modeled realistically from measured or computed data. Mathematically, it is an odd function and as such can be expanded in odd powers of the input voltage. The coefficients of the polynomial fit are calculated from a least-squares algorithm. The deviation from linearity arises, of course, from the thirds, fifths, etc., terms of the expression; and each additional term gives rise to a higher order intermodulation product. A problem arises in deciding where to truncate the series. From the point of view of the least-squares error the fit becomes better as higher order terms are included. However, with each additional term the expansion coefficients must be recalculated and will differ from previously calculated coefficients thus causing an ambiguity in the computation of intermodulation products. This is a consequence of the nonorthogonality of the power series. A method for removing the ambiguity consistent with the inherent error of the data is discussed in appendix A.

This paper is divided into a section called FORMULATION and one called RESULTS with most of the mathematical derivations relegated to appendixes

A, B, and C. The computer program is not given at this time but is demonstrated in the section RESULTS using the particular channel spacings of reference 3.

Formulation

Figure 1 is typical of a power gain curve for a TWT. The input and output powers have been normalized to their saturation values and the deviation from linearity (dashed line) is the gain compression (about 1.9 dB at saturation). This particular curve is the result of TWT computer simulation and was generated as part of a design study for the 75-watt, 20-gigahertz tube of reference 3.

The voltage transfer curve which is the square root of the power gain curve is shown in figure 2. The error associated with the data used in making this plot was judged to be ± 0.005 based on visually estimating the points in figure 1. The error would have been smaller had the raw computer data been used. However, experimental data is usually plotted and the experimental accuracy often is not given; hence, the error associated with a visual estimate is probably consistent with most generated data.

The method described in appendix A can be used to expand the vector of voltage transfer data in an orthogonal set of polynomials W_j

$$(V/V_{sat})_{output} = \sum_j b_j W_j \tag{1}$$

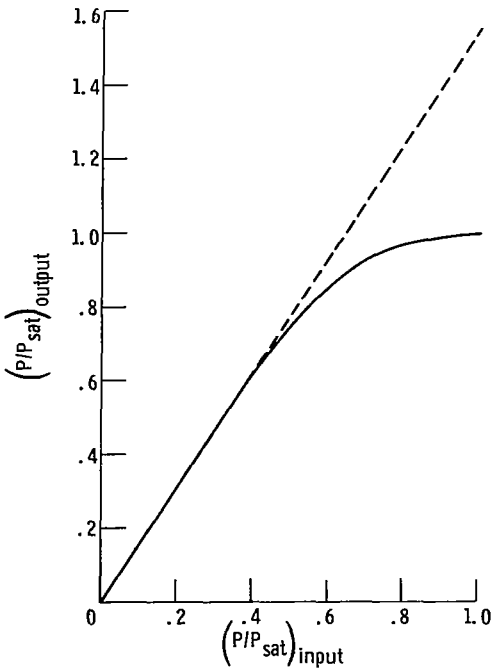

Figure 1. - Normalized power gain curve for a traveling wave tube.

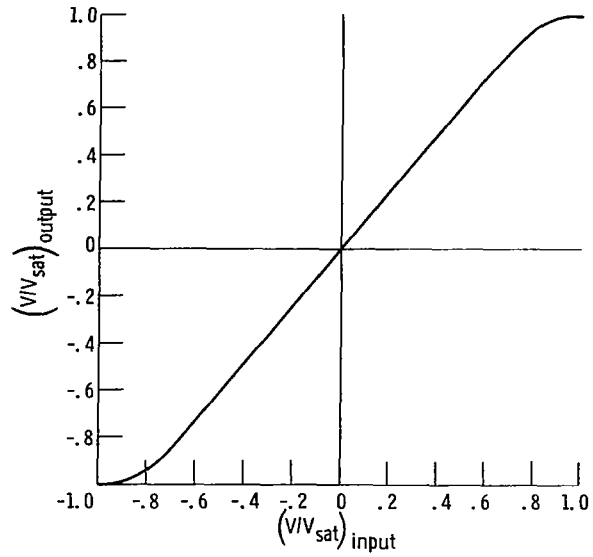

Figure 2. - Normalized voltage transfer curve for a traveling wave tube.

A computer program called POLYBASE was written to compute the orthogonal vectors W_j from the input vector data $(V/V_{sat})_{input}$ and to perform the scalar products that define the expansion coefficients b_j as follows:

$$b_j = (V/V_{sat}) \cdot W_j \tag{2}$$

The results obtained by using the data of figure 2 are given in table I for the first six coefficients. Only the first three coefficients fall within the error norm of 2.022×10^{-2} as calculated from this data using equation (A8). Therefore, the data should be fit with a fifth-order polynomial. By using a least-squares-error algorithm, the fifth-order polynomial fit of the data in figure 2 is found to be

$$y = 1.228x + 0.158x^3 - 0.386x^5 \tag{3}$$

TABLE I. - FIRST SIX SCALAR PRODUCTS OF OUTPUT DATA VECTOR (SEE FIG. 2) WITH ORTHOGONAL BASIS OF DATA VECTOR SPACE

b_1	3.145
b_2	-0.2430
b_3	-0.8118×10^{-1}
----------	Error norm $= 0.2022 \times 10^{-1}$
b_4	-0.3194×10^{-2}
b_5	0.9272×10^{-2}
b_6	0.1286×10^{-2}

where $y=(V/V_{sat})_{output}$ and $x=(V/V_{sat})_{input}$.

It will be assumed that equation (3) is valid when the input and output signals are functions of time. In general, the output signal appears at a time τ after introducing the input signal. That is, an output $y(t)$ will occur in response to an input $x(t+\tau)$. However, unless the time delay τ is a function of frequency, the Fourier transform of equation (3) will yield a constant and hence factorable phase for each term in the equation. The study of frequency dependent time delays is an interesting facet of nonlinear systems; however, as explained in the INTRODUCTION, they are beyond the scope of this paper.

Equation (3) can thus be rewritten as

$$y(t)=\sum_{k=1}^{3} c_{2k-1}x(t)^{2k-1} \tag{4}$$

The Fourier transform of equation (4) gives the following equivalent expression in the frequency domain (see eq. (B4)):

$$Y(f)=\sum_{k=1}^{3} c_{2k-1}X(f)^{\circledast(2k-1)} \tag{5}$$

The normalized output spectral power density from equation (B42) is

$$Y^2(f)=\sum_{k_1=1}^{3}\sum_{k_2=1}^{3} c_{2k_1-1}c_{2k_2-1}$$

$$\left[X(f)^{\circledast(2k_1-1)}X(f)^{\circledast(2k_2-1)}\ P_{(k_1,k_2)}\right]$$

where

$$P_{(k_1,k_2)}=\int_{-\infty}^{\infty} X_{sat}(f)^{\circledast(2k_1-1)}X_{sat}(f)^{\circledast(2k_2-1)}df \tag{6}$$

The input signal $X(f)$ to the nonlinear system is assumed to be a distributed rather than a line source. The distribution can be expanded in a series of Gaussian sources each having a width, that is, a standard deviation of $1/\sqrt{2}\lambda$ where λ is a convenient parameter to adjust the expansion. Equation (B13) or its integerized version (eq. (C24)) is the type of expansion that is supposed. Using only the positive frequencies from equation (B13) we have

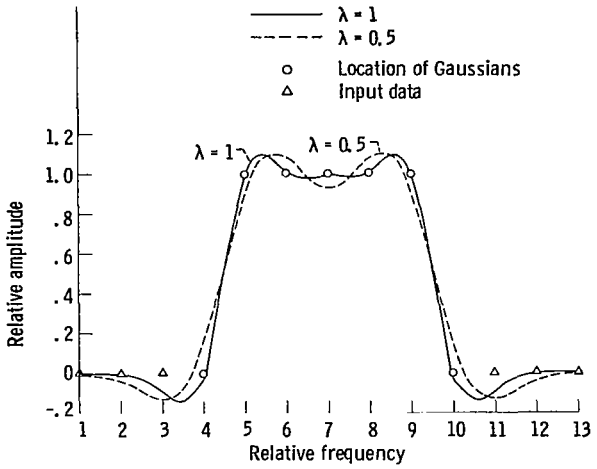

Figure 3. - Least-squares fit of a trapezoidal frequency gate using seven Gaussian functions.

$$X(f)=\sum_{n=1}^{N} a_n\, e^{-\lambda(f-f_n)^2} \tag{7}$$

Equation (7) is a linear expansion in N Gaussian functions each centered about a frequency f_n with the amplitudes a_n as the expansion coefficients. A linear regression with a least-squares technique can be used to find a_n for a given distribution. Figure 3 shows the results of such a computation for a trapezoidal frequency gate or bandpass filter. The gate is ideal and has unit amplitude at the discrete relative frequencies between 5 to 9 and zero amplitude elsewhere. The calculation was done for two values of the parameter λ. The solid curve with $\lambda=1$ has the smaller residual and therefore is chosen as the model of a bandpass filter. In the remainder of this paper the input driving signal to the nonlinear amplifier will be in the form of multiple channels defined by bandpass filter gates.

The amplitude coefficients a_n have, so far, been arbitrary and it is necessary to normalize them in order to compute the correct results. The input power P_i is defined by the integral

$$P_i=\int_{-\infty}^{\infty} X(f)^2\,df \tag{8}$$

Using equation (7) we get

$$P_i=\sum_{n_1=1}^{N}\sum_{n_2=1}^{N} a_{n_1}a_{n_2}\int_{-\infty}^{\infty} e^{-\lambda\left[\left(f-f_{n_1}\right)^2+\left(f-f_{n_2}\right)^2\right]}df \tag{9}$$

After rearranging terms and carrying out the integration, this becomes

$$P_i = \left(\frac{\pi}{2\lambda}\right)^{1/2} \sum_{n_1=1}^{N} \sum_{n_2=1}^{N} f_{n1} f_{n2} \, e^{-(\lambda/2)(f_{n_1} - f_{n_2})^2} \tag{10}$$

The scale factor S from equation (B39) can be used to rewrite equation (10) as

$$P_i = S^2 \left(\frac{\pi}{2\lambda}\right)^{1/2} \sum_{n_1=1}^{N} \sum_{n_2=1}^{N} (a_{n1})_{sat} (a_{n2})_{sat} \, e^{-(\lambda/2)(f_{n_1} - f_{n_1})^2}$$

$$= S^2 (P_i)_{sat} \tag{11}$$

Equation (11) becomes the defining equation for the scale factor S, which is equal to unity at saturation and less than one below saturation. The arbitrariness in the amplitude coefficients a_n is removed by redefining them as

$$a_n \rightarrow a_n / (P_i)_{sat}^{1/2} \tag{12}$$

A computer program was developed to calculate the output spectral density (eq. 5)) as a function of the input signal (eq. (7)). The program coding, which will not be presented, follows the logic outlined in appendix C. The coherent part of the spectral density Y_c^2 is computed from the terms given by equations (C24) to (C29). The noise density is then given by

$$Y_N^2 = Y^2 - Y_c^2 \tag{13}$$

The signal-to-noise ratio in the band between f_a and f_b is

$$(S/N)_{a,b} = \int_{f_a}^{f_b} Y_c^2(f)\, df \int_{f_a}^{f_b} Y_N^2(f)\, df \tag{14}$$

As an example, the program was used to analyze the signal-to-noise ratios of the multichannel inputs to a nonlinear TWT as proposed in reference 3. These computations are discussed in the following section.

Results

It was assumed in reference 3 that the total bandwidth available to a certain communications system was divided into nine separate channels of equal width (see fig. 4). The channels are delineated with ideal bandpass filters. It was further assumed that the transmitter would consist of three TWT amplifiers carrying three channnels each. The distribution of the three channels within each TWT was chosen so that the third-order intermodulation products would fall between the channels and could, therefore, be removed with filters after amplification.

Assigning channel numbers (as in fig. 4) means, the first TWT would carry channels 1, 3, and 7; the second TWT would carry channels 2, 4, and 8; and the third

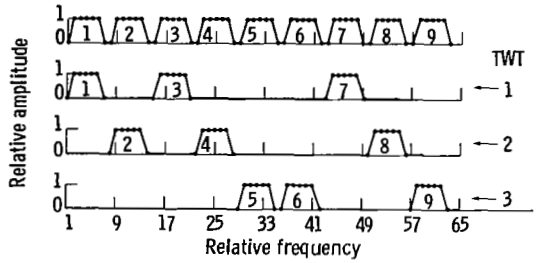

Figure 4. - Assumed distribution of nine channels over three traveling wave tubes (TWT's).

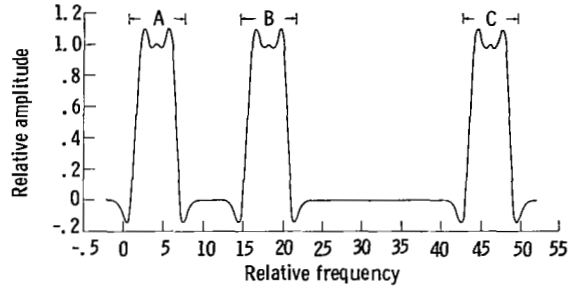

Figure 5. - Distribution of channels for case one.

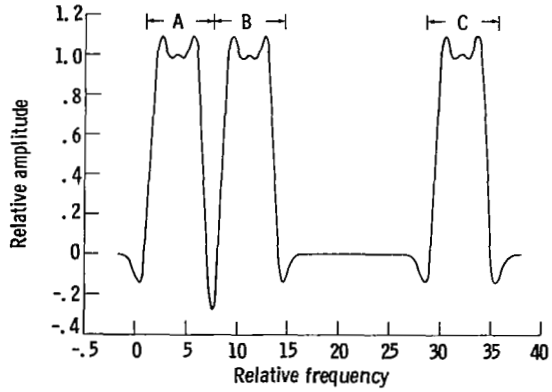

Figure 6. - Distribution of channels for case two.

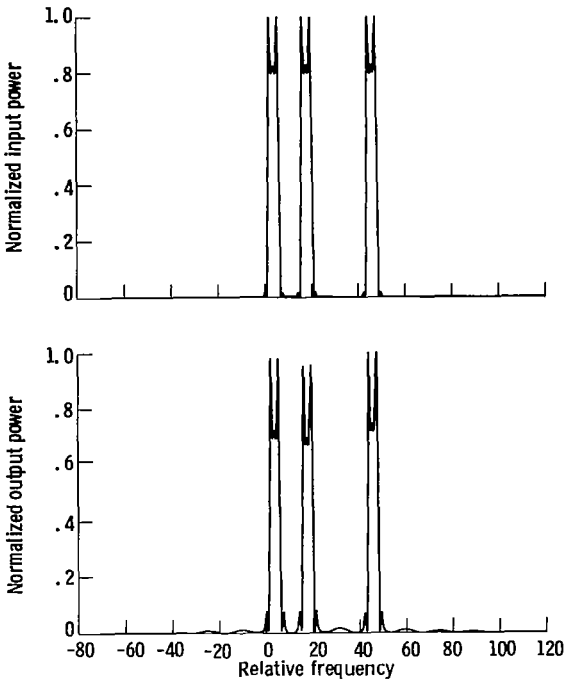

Figure 7. - Input and output powers at saturation for channel distribution of case one.

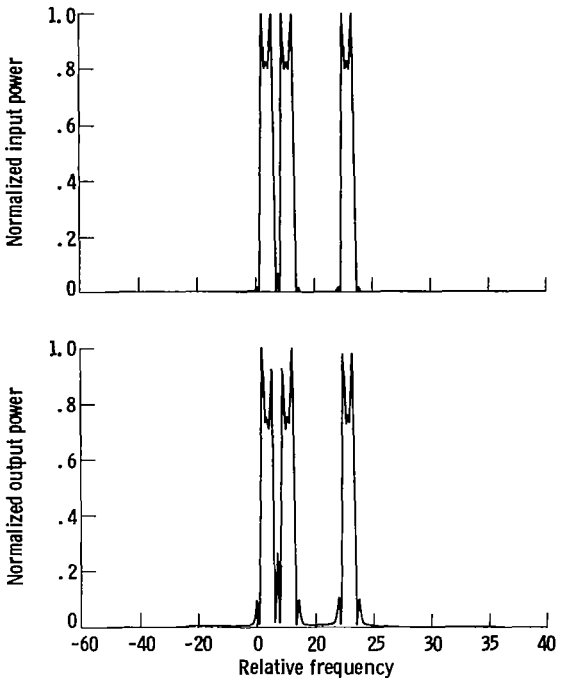

Figure 9. - Input and output powers at saturation for channel distribution of case two.

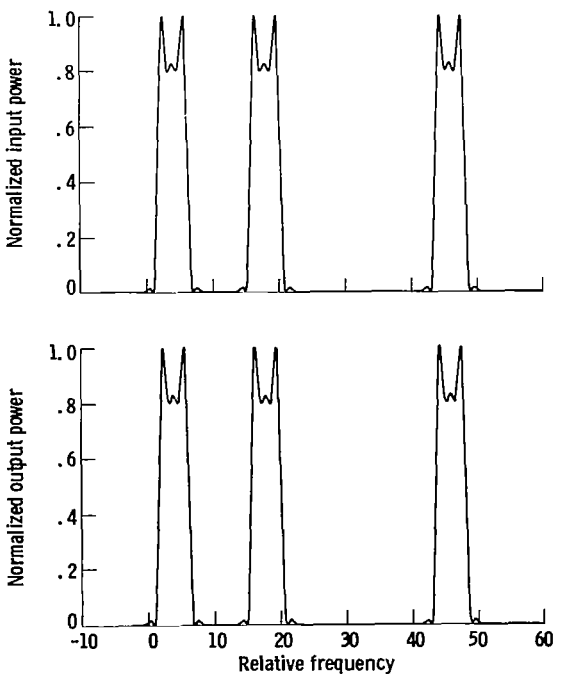

Figure 8. - Input and output powers at -4 dB from saturation for channel distribution of case one.

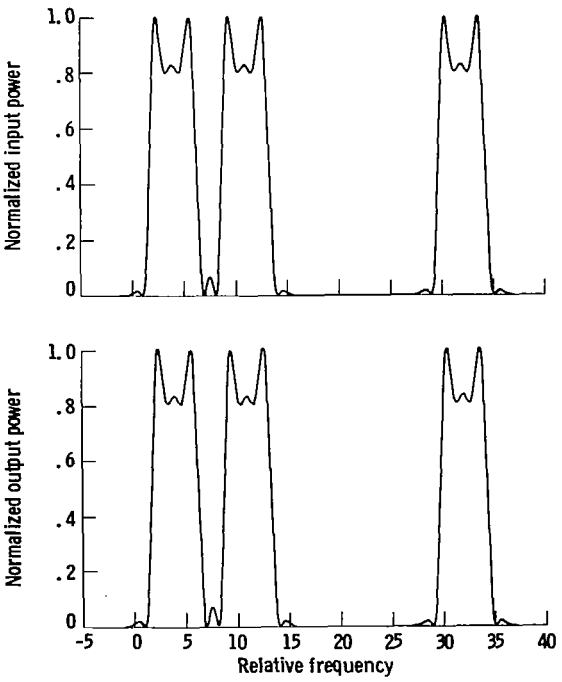

Figure 10. - Input and output powers at -4 dB from saturation for channel distribution of case two.

TWT would carry the remaining channels 5, 6, and 9. If it is assumed that the bandwidth of each TWT is uniform, then the channel distribution 1, 3, and 7 is identical to the distribution 2, 4, and 8. This is because the two arrangements are merely translations of each other and intermodulation products depend only on relative frequencies. Hence, in order to analyze this system only two distinct cases need be considered.

Figure 5 shows the distribution of channels, designated as case one, which is the representation in Gaussian functions of both of the arrangements (1, 3, 7) and (2, 4, 8). Figure 6 is the distribution for case two which is the

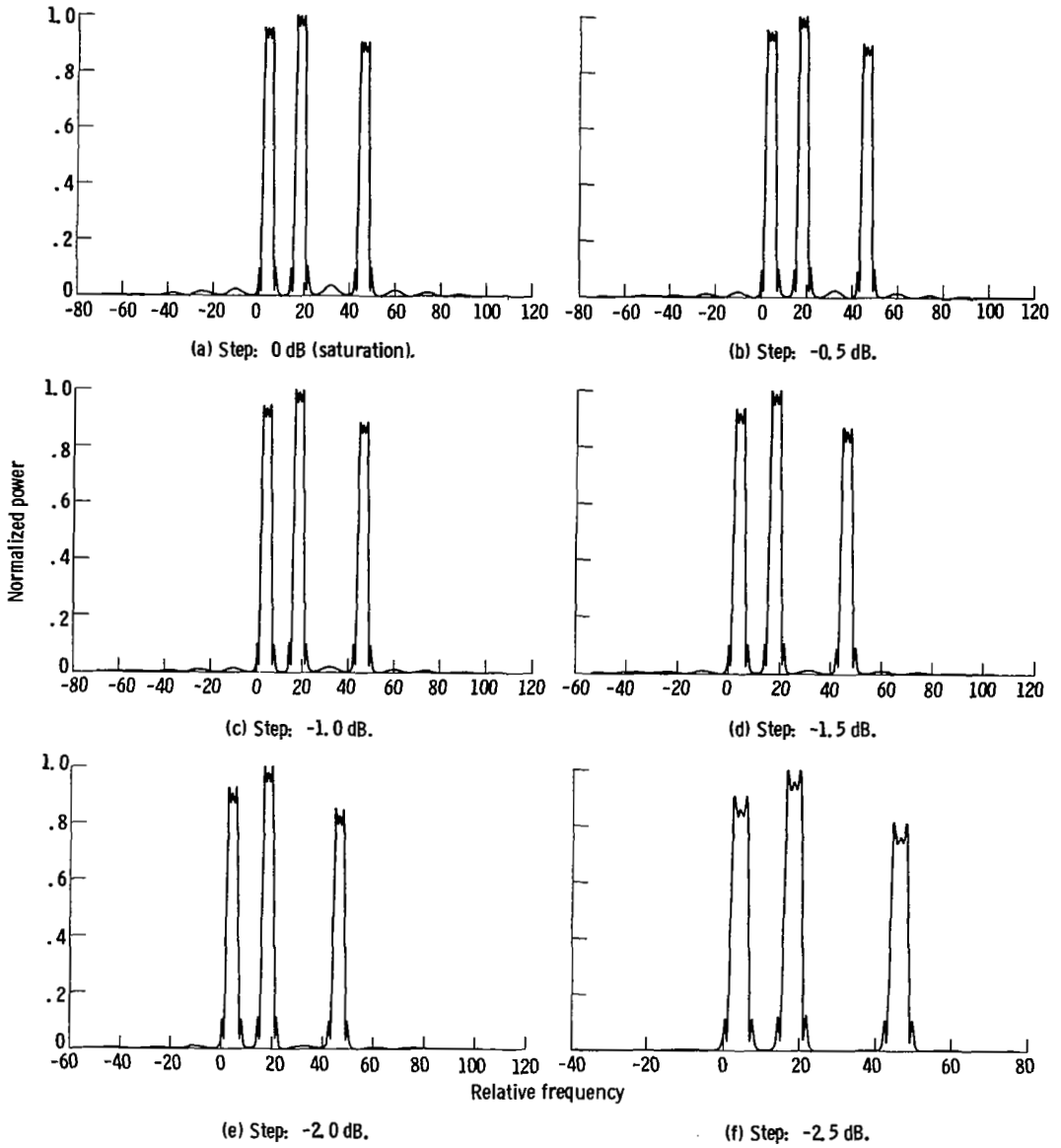

Figure 11. - Sequence of output noise power for channel distribution of case one in 1/2-dB steps from saturation to -5dB below saturation. Power is normalized to its peak for each step.

input representation for channels 5, 6, and 9. The three channels in each case are designated as channels A, B, and C.

Cases one and two were analyzed for a sequence of input powers ranging from saturation to −10 dB below saturation. The computer program uses a graphics package to display the input and the output spectral power density of the nonlinear amplifier. Figure 7 shows the power density of the input and the output at saturation for case one. As the drive power is decreased beyond −3 dB from saturation, the output intermodulation structure, although it is present, is

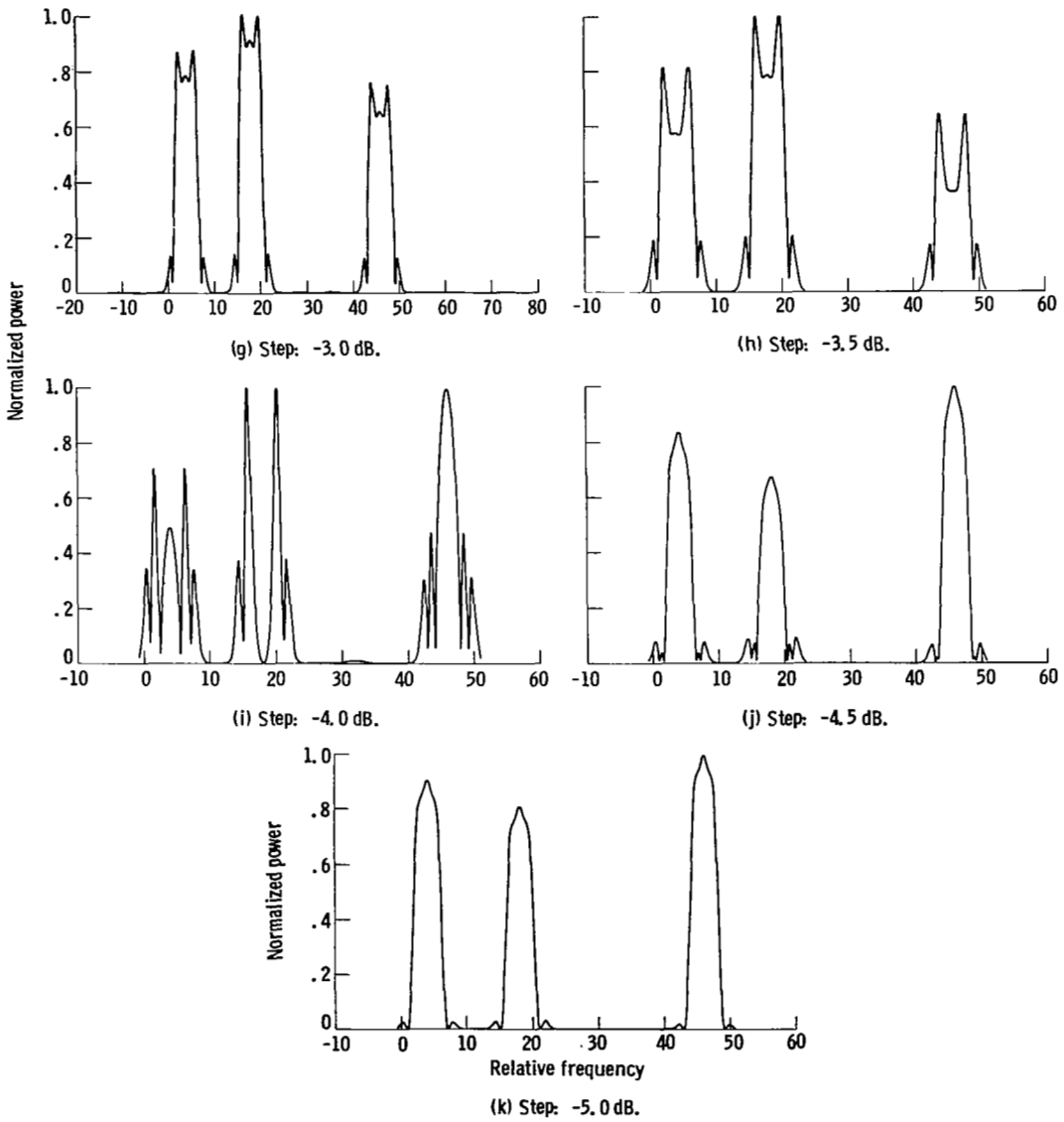

Figure 11. - Concluded.

scarcely discernible in the graphics display. The situation at −4 dB is given in figure 8 and shows that the output spectral density appears to be a replica of the input spectral density.

Figures 9 and 10 show the spectral density input and output power for case two. Figure 9 is the result at saturation and figure 10 is at −4 dB from saturation.

It is more interesting to have the computer produce a display of the noise spectral density rather than the total output spectral density. Figure 11 is a sequence of computer plots showing the noise density for case one in steps of 0.5 dB from saturation to −5 dB below saturation. Figure 12 is an identical sequence but for case two. Note that, between −3.5 and −4.5 dB below

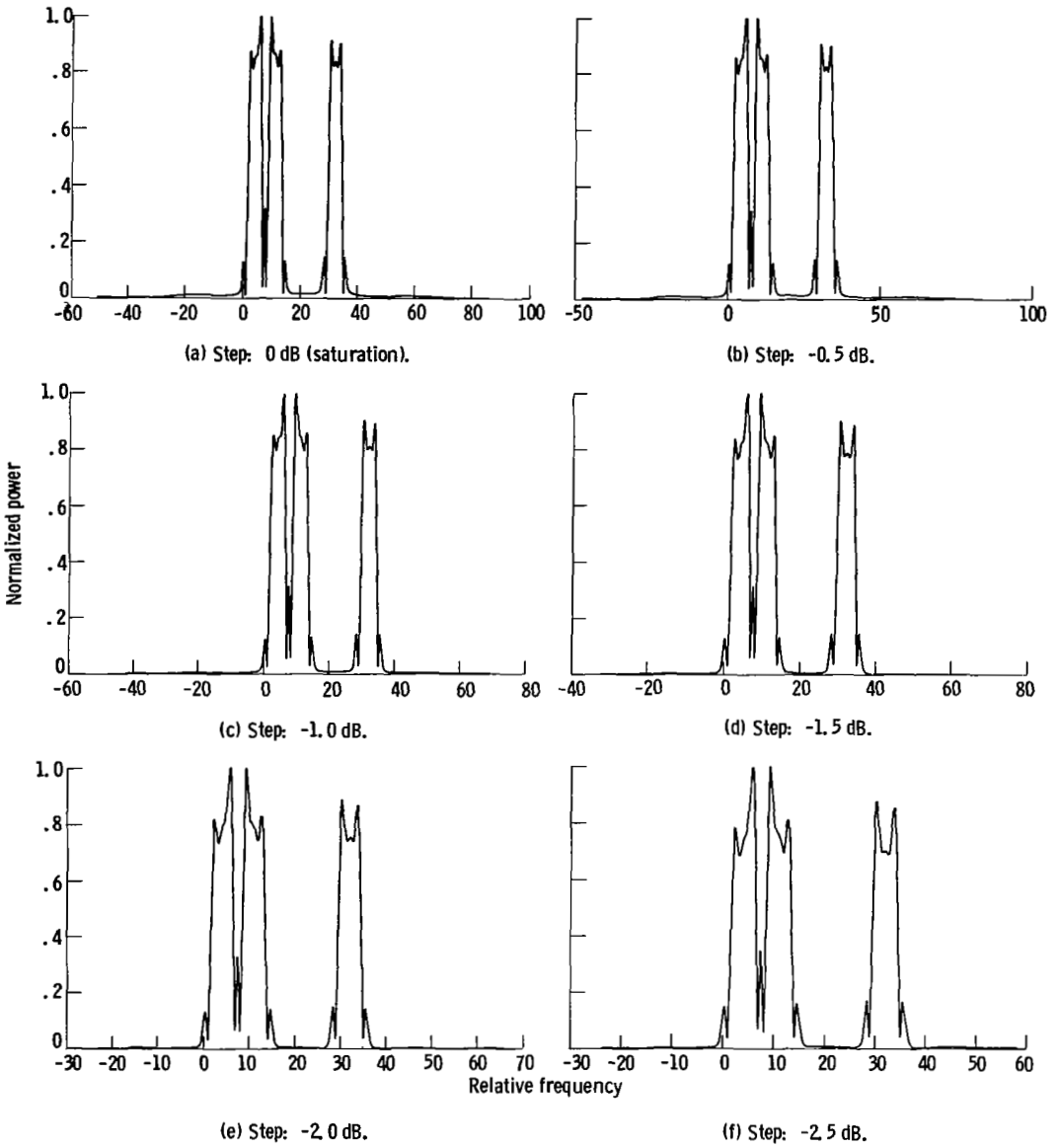

Figure 12. - Sequence of output noise power for channel distribution of case two in 1/2-dB steps from saturation to -5 dB below saturation. Power is normalized to its peak for each step.

saturation, a type of transition takes place in which the character of the noise changes. This behavior is a consequence of the particular voltage transfer function that was used in this example (see fig. 2). Because the least-squares fit to this curve (eq. (3)) has a positive third-order coefficient and a negative fifth-order coefficient there exists a region in which these two terms cancel. This occurs at

$$x^2 = \frac{0.158}{0.386} = 0.409 = -3.883 \text{ dB} \tag{15}$$

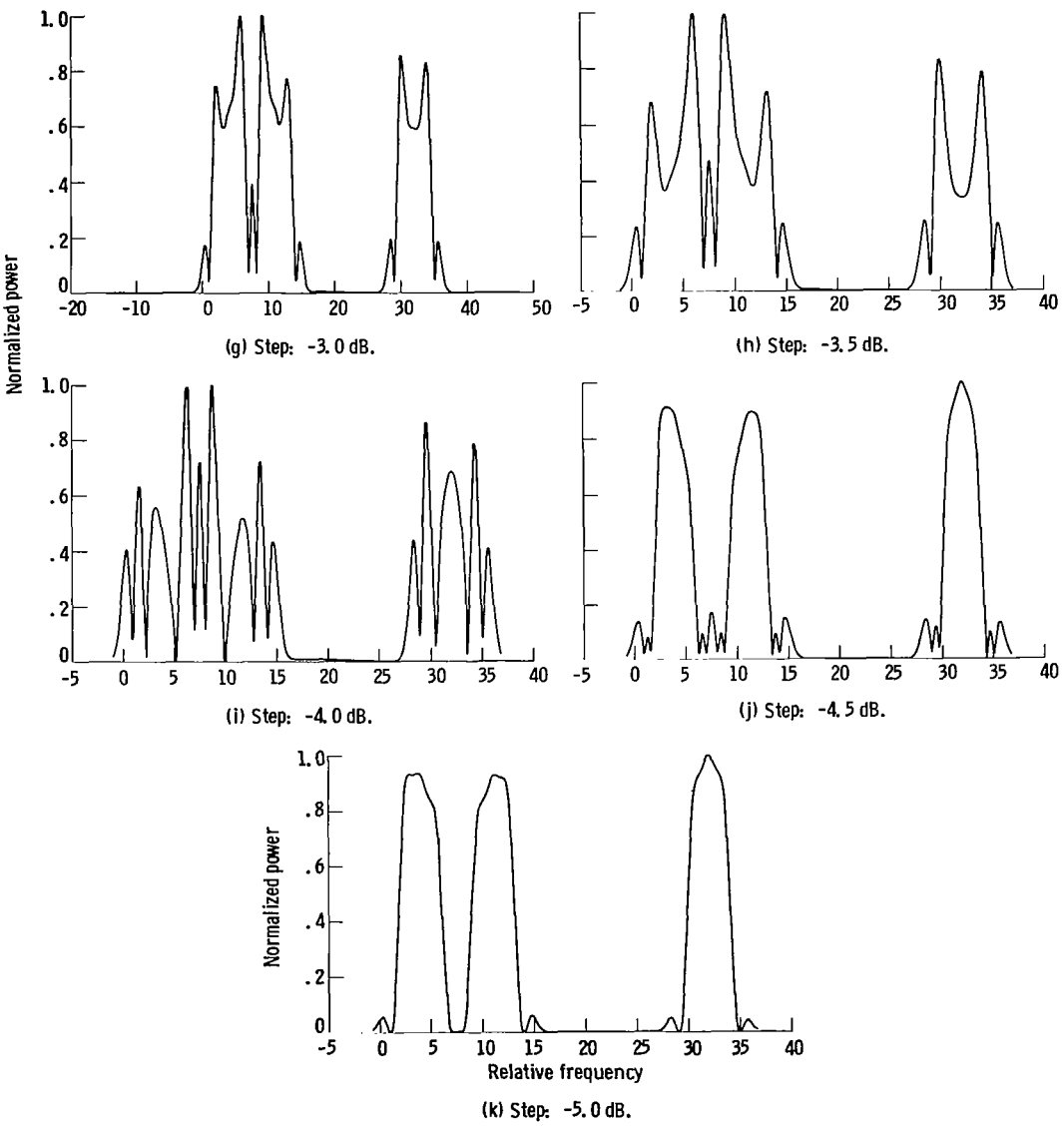

Figure 12. - Concluded.

Note that at saturation when $x = 1$ the fifth-order term is larger than the third-order term. Thus, the fifth-order terms dominate from saturation to the transition point (eq. (15)) and the third-order terms are dominant below this point.

The computer program provides the signal-to-noise ratio for each channel by calculating the integrals in equation (14). Figures 13 and 14 show the results of this computation for the channel distributions of cases one and two, respectively.

The most interesting feature of these plots is the apparent singularity at approximately the value given by equation (15). This was unexpected because equation (15) is the result of integrating over all frequencies while the signal-to-noise ratios involve local integrals over the band in which a channel is defined.

The numerical differences in signal-to-noise ratios between individual channels and even between the two cases are very slight. In figures 13 and 14 the line thicknesses bound the values for the various channels. If the two cases are superimposed, they coincide within these bounds. Evidently the signal-to-noise ratio is very dependent on the coefficients of the third- and fifth-order terms and the fact that in this case they differ in sign.

A hypothetical transfer curve in which both of these coefficients are negative was derived to study the same

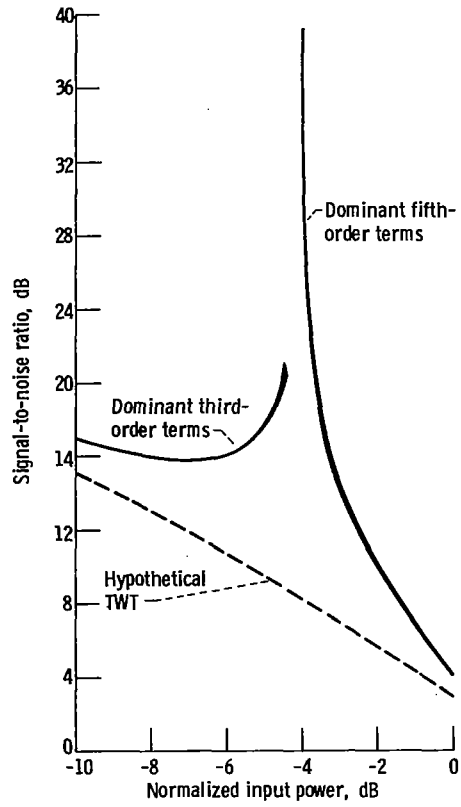

Figure 14. - Signal-to-noise ratio as a function of drive power for case two. (Individual channels are bounded by line thicknesses.)

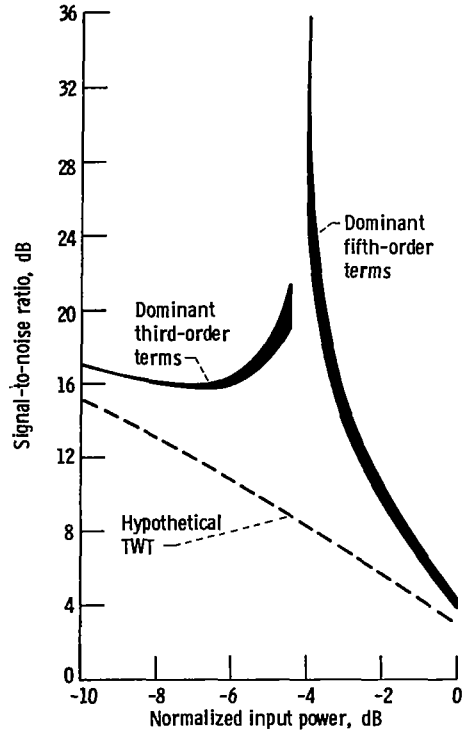

Figure 13. - Signal-to-noise ratio as a function of drive power for case one. (Individual channels are bounded by line thicknesses.)

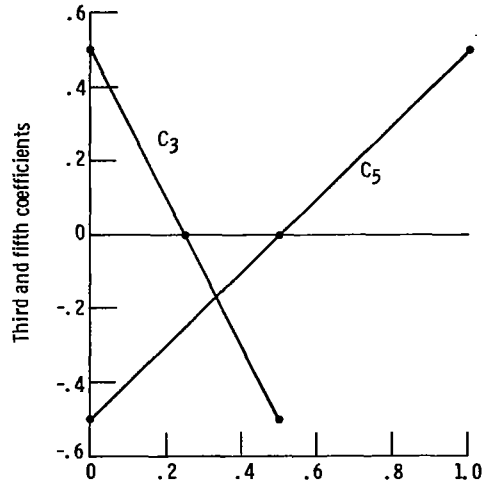

Figure 15. - Plot of third and fifth coefficients as functions of parameter ϵ.

channel distributions. The dashed lines in figures 13 and 14 show these results.

The voltage transfer curve shown in figure 2 has the general characteristics that

$$\left.\begin{aligned} y &= 1 \\ \frac{dy}{dx} &= 0 \end{aligned}\right\} \quad \text{at } x = \pm 1 \tag{16}$$

and

$$\frac{dy}{dx} > 1 \text{ at } x = 0$$

The first condition is a consequence of using a normalized transfer function while the second is the saturation characteristic. The third condition is a statement that for curves of single curvature one can never satisfy conditions (1) and (2) unless the coefficient of the linear term is greater than one. Using equation (4) and the conditions in equation (16) yields

$$\left.\begin{aligned} c_1 + c_3 + c_5 &= 1 \\ c_1 + c_3 + c_5 &= 0 \\ c_1 &= 1 + \epsilon, \ \epsilon > 0 \end{aligned}\right\} \tag{17}$$

These can be solved in terms of ϵ with the following result:

$$\left.\begin{aligned} c_3 &= 2\left[\left(\frac{1}{4}\right) - \epsilon\right] \\ c_5 &= \epsilon - \left(\frac{1}{2}\right) \end{aligned}\right\} \tag{18}$$

Obviously c_3 is always negative for ϵ greater than 1/4 and c_5 is always positive for ϵ greater than 1/2. However, both coefficients may be negative in the region

$$\frac{1}{4} < \epsilon < \frac{1}{2} \tag{19}$$

This region is shown in figure 15 where equations (18) are plotted. The values chosen for the hypothetical transfer function were

$$\left.\begin{aligned} c_1 &= 1.3333 \\ c_3 &= 0.1667 \\ c_5 &= 0.1667 \end{aligned}\right\} \tag{20}$$

However, the results shown in figures 13 and 14 indicate that the hypothetical case is noisier. Further investigations of the effect of the coefficients on the signal-to-noise ratio were deferred until a more complete study could be undertaken. Such an investigation would be of great help in designing TWT's with optimum low noise characteristics.

Concluding Remarks

The nonlinear power gain characteristic of a soft limiter such as a traveling wave tube (TWT) produces interchannel distortions if it is used as a multichannel amplifier. In order to minimize the effect of these distortions, it is necessary to operate the TWT quasi-linearly; that is, backed-off from saturation. With the help of a computer program which was developed for this problem, the signal-to-noise ratios are calculated for various distributions of channels as a function of driving power.

The nonlinear gain characteristic is represented as a power series in input signal voltage and a least-squares algorithm is used to fit the measured or computed gain data. A criterion for truncation of the series is developed which depends on the inherent error of the data. This criterion removes the ambiguities which results if an arbitrary truncation is used.

The input signal channels are modeled by linear regression theory in which measured or computed bandpass channel characteristics are fit with Gaussian functions. This procedure bypasses the ensemble averaging that is usually performed to specify the frequency bands required by a given channel. This also defers the need to consider signal coding, modulation and information recovery in the analysis.

Two specific distributions of channels are analyzed. It is found that the signal-to-noise ratios are very sensitive to the coefficients which are used in the power series expansion of the gain characteristic curve. The procedures described in this paper can be used in defining the optimum gain characteristics and drive levels for low noise, multichannel operation.

Lewis Research Center
National Aeronautics and Space Administration
Cleveland, Ohio, May 28, 1981.

Appendix A

Voltage Transfer Function (AM/AM) for a TWT

We assume that a measured or calculated power transfer curve is available. Figure 1 is typical of the nonlinear characteristics of such a calculated power transfer curve. The normalized output power is plotted in this figure as a function of the input or drive power. The normalization is with respect to saturation values.

The normalized voltage transfer function is derived by taking the square root of the power curve. This function is plotted in figure 2. Note that the voltage transfer function includes both the positive and negative roots of the power curve and that it is a completely odd function.

Because it is an odd function, the voltage transfer can be represented as a polynomial expansion using only odd terms. Defining $x(t)$ and $y(t)$ as the normalized input and output signal voltages yields

$$y(t)=\sum_{k=1}^{K} c_{2k-1}x(t)^{2k-1} \tag{A1}$$

The limit on the summation K is the order of the truncation of the representation. For example, $K=5$ will truncate the series at the ninth power of the input and this will, of course, result in ninth-order intermodulation products.

One way of determining the coefficients (c_1, c_3, c_5, . . . , c_{2K-1}) is to apply, directly, a least-squares polynomial fit to equation (A1). Let the data, taken from the voltage transfer curve, be designated as

$$y_i=y(x_i) \tag{A2}$$

where i ranges over the number of data points used in the fit.

The sum of the square of the residuals, derived from equation (A1) and regarded as a function of the coefficients, is

$$\epsilon(c_1,c_3,\ldots)=\sum_i\left(y_i-\sum_{k=1}^{K} c_{2k-1}x_i^{2k-1}\right)^2 \tag{A3}$$

The condition that the sum of residuals be a minimum is expressed as

$$\frac{\partial\epsilon}{\partial c_l}=0; \qquad l=1,\ldots,K \tag{A4}$$

Equation (A4) leads to a set of N linear equations which, with some matrix manipulations, can be solved for the coefficients c_l. Unfortunately, this method of determining the coefficients tells nothing about the number of terms required for the representation. That is, the final degree of the polynomial is arbitrary.

The computed deviations from the data show that the fit becomes better as more terms are considered. However, the coefficients c_k change with the addition of each new term. This leads to ambiguous results in which each representation gives a different value for the intermodulation products. In some radical cases the higher order products are more pronounced than the lower orders. This cannot be an adequate description of a real nonlinear amplifier.

In order to set a limit to the number of required terms, some account must be taken of the quality of data used. To begin, equation (A1) can be written as the following vector expansion in polynomial space:

$$\begin{pmatrix} y_1 \\ y_2 \\ \cdot \\ \cdot \\ \cdot \\ y_n \end{pmatrix} = c_1 \begin{pmatrix} x_1 \\ x_2 \\ \cdot \\ \cdot \\ \cdot \\ x_n \end{pmatrix} + c_3 \begin{pmatrix} x_1^3 \\ x_2^3 \\ \cdot \\ \cdot \\ \cdot \\ x_n^3 \end{pmatrix} + c_5 \begin{pmatrix} x_1^5 \\ x_2^5 \\ \cdot \\ \cdot \\ \cdot \\ x_n^5 \end{pmatrix} + \ldots \tag{A5}$$

The components of the vectors are the n data points read from figure 2. We will assume that the x_i data is exact and that each y_i point has an associated error Δy_i. The norm of the y vector is defined by

$$N_y=\sum_{i=1}^{n} y_i^2 \;^{1/2} \tag{A6}$$

The norm gives the length of a vector in the n-dimensional space in which it is imbedded, and it is an invariant with respect to coordinate transformations.

However, because of the errors Δy_i there is an uncertainty in the vector y

$$N_y+\Delta N_y=\left[\sum_{i=1}^{n}(y_i+\Delta y_i)^2\right]^{1/2}$$
$$=f(\Delta y_1\ldots\Delta y_n) \tag{A7}$$

In the last expression we concentrate on the norm as a function f of the errors Δy_i. Expanding f in a multivariable Taylor series in Δy_i and ignoring terms higher than first order result in

$$N_y + \Delta N_y = f_0 + \left(\frac{\partial f}{\partial \Delta y_1}\right)_0 \Delta y_1 + \ldots + \left(\frac{\partial f}{\partial \Delta y_n}\right)_0 \Delta y_n$$

$$= N_y + \left(\frac{1}{N_y}\right)[y_1 \Delta y_1 + \ldots + y_n \Delta y_n]$$

$$\Delta N_y = \left(\frac{1}{N_y}\right) \sum_{i=1}^{n} y_i \Delta y_i$$

This can be written as a scalar product of two vectors

$$\Delta N_y = \left(\frac{1}{N_y}\right) y \bullet e \tag{A8}$$

where

$$e = \begin{pmatrix} \Delta y_1 \\ \cdot \\ \cdot \\ \cdot \\ \Delta y_n \end{pmatrix} \tag{A9}$$

The relationship in equation (A8) is pictured geometrically in figure 16.

The problem is to resolve the vector y into its components along a coordinate system which spans the n-dimensional space. That is, we wish to find the subspace in which to expand y. We assume that all n vectors are not necessary. Furthermore, any component of y having a value less than the error in the norm of y will be considered ignorable. We proceed by defining

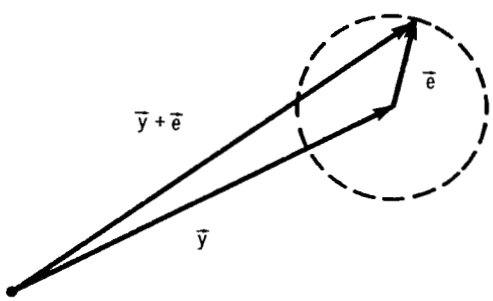

Figure 16. - Geometrical relationship between data vector $\bar{y}$ and error vector $\bar{e}$.

$$\left.\begin{aligned} X_1 &= (x_1 \ldots x_n)^T, \quad a_1 = c_1 \\ X_2 &= (x_1^3 \ldots x_n^3)^T, \quad a_2 = c_3 \\ X_3 &= (x_1^5 \ldots x_n^5)^T, \quad a_3 = c_5 \\ \text{etc.} & \qquad\qquad \text{etc.} \end{aligned}\right\} \tag{A10}$$

where T denotes the transpose. Then, equation (A5) is rewritten as

$$y = \sum_i a_i X_i \tag{A11}$$

The set of vectors X_i span the entire space. Unfortunately, they are not orthogonal. Basically, this is the reason they are not convenient in finding the subspace of y.

An orthogonal set of coordinates can be constructed using the Gram-Schmidt orthogonalization method. Let $(W_1, W_2, \ldots)$ denote the orthogonal set given by

$$\left.\begin{aligned} W_1 &= X_1 \\ W_2 &= X_2 - \frac{X_2 \bullet W_1}{W_1 \bullet W_1} W_1 \\ W_3 &= X_3 - \frac{X_3 \bullet W_1}{W_1 \bullet W_1} - \frac{X_3 \bullet W_2}{W_2 \bullet W_2} W_2 \\ \text{etc.} & \end{aligned}\right\} \tag{A12}$$

The data vector y can now be expanded in the orthogonal set as

$$y = \sum_i b_i W_i \tag{A13}$$

in which the expansion coefficients are given by

$$b_j = y \bullet W_j \tag{A14}$$

and the right side is the scalar product of y and W_j. Finally, we impose the condition that

$$b_j > \Delta N_y \tag{A15}$$

and we reject all b's which are less than ΔN_y.

Using this procedure we can define the subspace in which y lies. This also defines, because of equation (A12), the highest order polynomial with which to apply the least-squares fit of equation (A4).

Appendix B

Spectral Distribution of the Voltage Transfer Function and Normalization of the Spectral Power Density Function

We assume that a normalized voltage transfer function (see eq. (A1)) has been found by least-squares fitting to a truncated polynomial series. It is also assumed that the truncation of the series is consistent with the inherent error of the data.

Taking the Fourier Transform of equation (A1) results in

$$Y(f) \equiv F\{y(t)\} = \sum_{k=1}^{K} c_{2k-1} F\{x(t)^{2k-1}\} \tag{B1}$$

where

$$F\{y(t)\} = \int_{-\infty}^{\infty} e^{-j2\pi ft} y(t)dt \tag{B2}$$

denoting

$$X(f) = F\{x(t)\} \tag{B3}$$

We note that the Fourier transform of a product in the t-domain is a convolution integral of the transform in the f-domain. Hence,

$$F\{X^2(t)\} = \int_{-\infty}^{\infty} X(f-s_1)X(s_1)ds_1 \equiv X(f) \circledast X(f)$$

and

$$F\{X^3(t)\} = \int_{-\infty}^{\infty}\int_{-\infty}^{\infty} X(f-s_1)X(s_1-s_2)X(s_2)ds_1 ds_2$$

$$= X(f) \circledast X(f) \circledast X(f)$$

$$\equiv X(f)^{\circledast 3}$$

With this notation equation (B1), the voltage spectral density, becomes

$$Y(f) = \sum_{k=1}^{K} c_{2k-1} X(f)^{\circledast(2k-1)} \tag{B4}$$

The integral of the spectral density over all frequencies can be carried out symbolically and the convolution integrals occurring in equation (B4) can be reduced to single integrations. Let

$$E_y \equiv \int_{-\infty}^{\infty} Y(f)df$$

Then

$$E_y = \sum_{k=1}^{K} c_{2k-1} \int_{-\infty}^{\infty} X(f)^{\circledast(2k-1)}\, df \tag{B6}$$

For notational clarity we change the variable of integration to s_1; then the multiple integrations become

$$\int_{-\infty}^{\infty} X(s_1)^{\circledast(2k-1)}\, ds_1$$

$$= \int_{-\infty}^{\infty} \cdots \int_{-\infty}^{\infty} X(s_1 - s_2)X(s_2 - s_3) \cdots$$

$$\times X(s_{2k-1})ds_1 \cdots ds_{2k-1} \tag{B7}$$

The variables of integration are now changed using the following transformation:

$$\left.\begin{aligned} s_1 &= u_1 + u_2 + \cdots + u_{2k-1} \\ s_2 &= u_1 + u_2 + \cdots + u_{2k-2} \\ &\vdots \\ s_{2k-1} &= u_1 \end{aligned}\right\} \tag{B8}$$

The Jacobian of this transformation is unity; therefore,

$$ds_1 \ldots ds_{2k-1} = du_1 \ldots du_{2k-1} \tag{B9}$$

and equation (B7) becomes

$$\int_{-\infty}^{\infty} X(s_1)^{\circledast(2k-1)}\, ds_1$$

$$= \int_{-\infty}^{\infty} \cdots \int_{-\infty}^{\infty} X(u_{2k-1}) X(u_{2k-2}) \cdots$$

$$\times X(u_1) du_{2k-1} \cdots du_1$$

$$= \int_{-\infty}^{\infty} X(u_{2k-1}) du_{2k-1}$$

$$\times \int_{-\infty}^{\infty} X(u_{2k-2}) du_{2k-2} \cdots$$

$$\times \int_{-\infty}^{\infty} X(u_1) du_1$$

$$= \left(\int_{-\infty}^{\infty} X(f) df \right)^{2k-1} \tag{B10}$$

The last step, leading to equaton (B10), results from the recognition that all the variables of integration $u_1 \ldots u_{2k-1}$ are dummy variables and can be replaced by f. Equation (B6) can now be written as

$$E_y = \sum_{k=1}^{K} c_{2k-1} E_x^{2k-1} \tag{B11}$$

with

$$E_x \equiv \int_{-\infty}^{\infty} X(f) df \tag{B12}$$

In order to proceed further with the spectral analysis, it is necessary to assume a particular form for $X(f)$. We will assume that the input signal (double-sided, i.e., both positive and negative frequencies) is

$$X(f) = \sum_{n=1}^{K} a_n \left[e^{-\lambda(f-f_n)^2} + e^{-\lambda(f+f_n)^2} \right] \tag{B13}$$

This form assumes N Gaussian signals having amplitude a_n and centered about f_n. Each signal has a standard deviation of $1/\sqrt{2}\lambda$. By letting the index n range from $-N$ to N (exclusive of zero) and allowing the convention

$$\left.\begin{aligned} a_{-n} &= a_n \\ f_{-n} &= -f_n \end{aligned}\right\} \tag{B14}$$

equation (B13) can be rewritten more compactly as

$$X(f) = \sum_{n=-N}^{N}{}' a_n e^{-\lambda(f-f_n)^2} \tag{B15}$$

The prime on the summation will be taken to mean that $n=0$ is excluded from the sum. The signal $x(t)$ in the time domain corresponding to equation (B15) is found by taking the inverse Fourier transform F^{-1} of $X(f)$ and is

$$x(t) = F^{-1}[X(f)]$$

$$= \int_{-\infty}^{\infty} X(f)\, e^{j2\pi ft} df$$

$$= 2\left(\frac{\pi}{\lambda}\right)^{1/2} e^{-(\pi^2/\lambda)t^2} \sum_{n=1}^{N} a_n \cos 2\pi f_n t \tag{B16}$$

Hence, the spectral distribution of equation (B15) results from applying the input signal of equation (B16) which is the application of N carriers for an effective duration, namely,

$$-\left(\frac{\sqrt{\lambda}}{\pi}\right) < t < \left(\frac{\sqrt{\lambda}}{\pi}\right) \tag{B17}$$

Here the effective duration is arbitrarily defined by the e-folding distance of the Gaussian time function. In fact, the duration is infinite.

The response of the nonlinear system in the frequency domain is given by equation (B4) with equation (B15) as the input. In order to determine the general form of the $2K-1$ convolution integrals which are needed we will proceed with the calculation of the third-order convolution. Thus

$$X(s_1)^{\circledast 3} = \sum_{n_1=-N}^{N}{}' \sum_{n_2=-N}^{N}{}' \sum_{n_3=-N}^{N}{}' a_{n_1} a_{n_2} a_{n_3}$$

$$\times \int_{-\infty}^{\infty} \int_{-\infty}^{\infty} e^{-\lambda G(s_1, s_2, s_3)} ds_2 ds_3 \tag{B18}$$

where

$$G(s_1,s_2,s_3)=(s_1-s_2-f_{l_1})^2+(s_2-s_3-f_{l_2})^2+(s_3-f_{l_3})^2 \quad \text{(B19)}$$

Using the following transformation:

$$\left.\begin{aligned} s_1 &= u_1+f_{n_1}+f_{n_2}+f_{n_3} \\ s_2 &= u_2+f_{n_2}+f_{n_3} \\ s_3 &= u_3+f_{n_3} \end{aligned}\right\} \quad \text{(B20)}$$

for which

$$ds_2 ds_3 = du_2 du_3$$

results in

$$G(u_1,u_2,u_3)=(u_1-u_2)^2+(u_2-u_3)^2+u_3^2 \quad \text{(B21)}$$

which can be written

$$G(u_1,u_2,u_3)=2\left(u_3-\frac{1}{2}u_2\right)^2+\frac{3}{2}\left(u_2-\frac{2}{3}u_1\right)^2+\frac{1}{3}u_1^2 \quad \text{(B22)}$$

Transforming variables again

$$\left.\begin{aligned} w_1 &= u_1 \\ w_2 &= u_2-\frac{2}{3}u_1 \\ w_3 &= u_3-\frac{1}{2}u_2 \end{aligned}\right\} \quad \text{(B23)}$$

for which

$$dw_2 dw_3 = du_2 du_3$$

yields

$$G(w_1,w_2,w_3)=2w_3^2+\frac{3}{2}w_2^2+\frac{1}{3}w_1^2 \quad \text{(B24)}$$

This procedure can be generalized for the higher order convolutions. The fifth order, for instance, is

$$G(w_1,w_2,w_3,w_4,w_5)=\frac{2}{1}w_5^2+\frac{3}{2}w_4^2+\frac{4}{3}w_3^2+\frac{5}{4}w_2^2+\left(1-\frac{4}{5}\right)w_1^2 \quad \text{(B25)}$$

and the seventh order becomes

$$G^{(7)}=\frac{2}{1}w_7^2+\frac{3}{2}w_6^2+\frac{4}{3}w_5^2+\frac{5}{4}w_4^2+\frac{6}{5}w_3^2+\frac{7}{6}w_2^2+\left(1-\frac{6}{7}\right)w_1^2 \quad \text{(B26)}$$

It is clear how the higher orders can be transformed. The integrals in equation (B18), the third-order convolution, become

$$\begin{aligned} &\int_{-\infty}^{\infty}\int_{-\infty}^{\infty} e^{-\lambda G(s_1 s_2,s_3)}\,ds_2\,ds_3 \\ &\quad = e^{-(\lambda/3)w_1^2}\int_{-\infty}^{\infty} e^{-2\lambda w_3^2}\,dw_3 \\ &\qquad \times \int_{-\infty}^{\infty} e^{-(3/2)\lambda w_2^2}\,dw_2 \\ &\quad = \left(\frac{1}{2\lambda}\right)^{1/2}\left(\frac{2}{3\lambda}\right)^{1/2} e^{(\lambda/3)w_1^2}\left(\int_{-\infty}^{\infty} e^{-\eta^2}\,d\eta\right)^2 \\ &\quad = \left(\frac{1}{2\lambda}\right)^{1/2}\left(\frac{2}{3\lambda}\right)^{1/2} e^{-(\lambda/3)w_1^2}(\sqrt{\pi})^2 \\ &\quad = \left(\frac{\pi}{\lambda}\right)\frac{1}{\sqrt{3}}\, e^{-(\lambda/3)w_1^2} \end{aligned} \quad \text{(B27)}$$

The integrals for the fifth order become

$$\int_{-\infty}^{\infty}\int_{-\infty}^{\infty}\int_{-\infty}^{\infty}\int_{-\infty}^{\infty} e^{-\lambda G(s_1,s_2,s_3,s_4,s_5)}\, ds_2\, ds_3\, ds_4\, ds_5$$

$$= e^{-(\lambda/5)w_1^2}\int_{-\infty}^{\infty} e^{-2\lambda w_5^2}\, dw_5 \int_{-\infty}^{\infty} e^{-(3/2)\lambda w_4^2}\, dw_4$$

$$\times \int_{-\infty}^{\infty} e^{-(4/3)\lambda w_3^2} dw_3 \int_{-\infty}^{\infty} e^{-(5/4)\lambda w_2^2} dw_2$$

$$= \left(\frac{1}{2\lambda}\right)^{1/2}\left(\frac{2}{3\lambda}\right)^{1/2}\left(\frac{3}{4\lambda}\right)^{1/2}\left(\frac{4}{5\lambda}\right)^{1/2}$$

$$\times (\sqrt{\pi})^4\, e^{-(\lambda/5)w_1^2}$$

$$= \frac{1}{\sqrt{5}}\left(\frac{\pi}{\lambda}\right)^2 e^{-(\lambda/5)w_1^2} \tag{B28}$$

And the multiple integrals from the seventh order become

$$\int_{-\infty}^{\infty}\cdots\int_{-\infty}^{\infty} e^{-\lambda G^{(7)}}\, ds_2 \ldots ds_7$$

$$= \left(\frac{1}{\sqrt{7}}\right)\left(\frac{\pi}{\lambda}\right)^3 e^{-(\lambda/7)w_1^2} \tag{B29}$$

Finally we list the convolutions of various order needed for the evaluation of equation (B4). In these expressions we have resubstituted variables according to $w_1 = u_1 = f - f_{n_1} + f_{n_2} + \ldots + f_{n_K}$ where K is the Kth convolution. Thus

$$X(f) = \sum_{n_1=-N}^{N}{}' a_{n_1} e^{-\lambda(f-f_{n_1})^2} \tag{B30}$$

$$X(f)^{\circledast 3} = \frac{1}{\sqrt{3}}\frac{\pi}{\lambda}\sum_{n_1=-N}^{N}{}'\sum_{n_1=-N}^{N}{}'\sum_{n_3=-N}^{N}{}' a_{n_1}a_{n_2}a_{n_3}$$

$$\times e^{-\frac{\lambda}{3}\left[f-(f_{n_1}+f_{n_2}+f_{n_3})\right]^2} \tag{B31}$$

$$X(f)^{\circledast 5} = \frac{1}{\sqrt{5}}\left(\frac{\pi}{\lambda}\right)^2 \sum_{n_1=-N}^{N}{}' \cdots \sum_{n_5=-N}^{N}{}' a_{n_1}\ldots a_{n_5}$$

$$\times e^{-\frac{\lambda}{5}\left[f-(f_{n_1}+\ldots+f_{n_5})\right]^2} \tag{B32}$$

$$X(f)^{\circledast 7} = \frac{1}{\sqrt{7}}\left(\frac{\pi}{\lambda}\right)^3 \sum_{n_1=-N}^{N}{}' \cdots \sum_{n_7=-N}^{N}{}' a_{n_1}\ldots a_{n_7}$$

$$\times e^{-\frac{\lambda}{7}\left[f-(f_{n_1}+\ldots+f_{n_7})\right]^2} \tag{B33}$$

And in general the Kth convolution is

$$X(f)^{\circledast K} = \frac{1}{\sqrt{K}}\left(\frac{\pi}{\lambda}\right)^{\frac{K-1}{2}} \sum_{n_1=-N}^{N}{}' a_{n_1} \cdots \sum_{n_K=-N}^{N}{}' a_{n_K}$$

$$\times e^{-\frac{\lambda}{K}\left[f-(f_{n_1}+\ldots+f_{n_K})\right]^2} \tag{B34}$$

The evaluation of these multiple sums is the subject of appendix C. As a final note we observe that the integration over all frequencies will yield the same results as in equation (B10).

The final topic of this appendix is the normalization of the spectral power density function. By definition the square of equation (B4) is the spectral power density; that is,

$$Y^2(f) = \sum_{k_1=1}^{K}\sum_{k_2=1}^{K} c_{2k_1-1}c_{2k_2-1}$$

$$X(f)^{\circledast(2k_1-1)}X(f)^{\circledast(2k_2-1)} \tag{B35}$$

Referring to equation (B11) note that at saturation E_x and E_y are both unity because the voltage transfer curve (fig. 2) has been normalized. Therefore,

$$\sum_{k=1}^{K} c_{2k-1} = 1 \tag{B36}$$

The power gain curve of figure 1 must be derivable from the spectral power density by integrating over all frequencies; thus,

$$\int_{-\infty}^{\infty} Y^2(f)df = \sum_{k_1=1}^{K} \sum_{k_2=1}^{K} c_{2k_1-1}c_{2k_2-1} \int_{-\infty}^{\infty} X(f)^{\circledast(2k_1-1)} X(f)^{\circledast(2k_2-1)} df \quad \text{(B37)}$$

Because the voltage transfer curve was derived by taking the square root of the power curve, equation (B37) must be expressible as a perfect square having the following form:

$$\int_{-\infty}^{\infty} Y^2(f)df = \left(\sum_{k=1}^{K} c_{2k-1}\beta^{2k-1} \right)^2 \quad \text{(B38)}$$

At saturation $\beta = 1$ and, therefore, the right side is equal to one.

The convolutions in equation (B37) can be expressed in terms of the convolution of saturation by means of a scale factor S; that is,

$$X(f)^{\circledast K} = S^K X_{sat}(f)^{\circledast K} \quad \text{(B39)}$$

This is most easily seen by recalling the origination of these terms

$$X(f)^{\circledast K} = F\{x^K(t)\} = S^K F\{x_{sat}^K(t)\} \quad \text{(B40)}$$

With these scale factors equation (B37) can be written as

$$\int_{-\infty}^{\infty} Y^2(f)df = \sum_{k_1=1}^{K} \sum_{k_2=1}^{K} c_{2k_1-1}c_{2k_2-1} S^{2(k_1+k_2-1)} \times \int_{-\infty}^{\infty} X_{sat}(f)^{\circledast(2k_1-1)} X_{sat}(f)^{\circledast(2k_2-1)} df \quad \text{(B41)}$$

In order that equation (B41) be reducible to the perfect square form of equaton (B38), it is clear that each term of the expression for $Y^2(f)$ be normalized by the integral of the term at saturation. Hence,

$$Y^2(f) = \sum_{k_1=1}^{K} \sum_{k_2=1}^{K} c_{2k_1-1}c_{2k_2-1} \times \left[X(f)^{\circledast(2k_1-1)} X(f)^{\circledast(2k_2-1)} \Big/ \int_{-\infty}^{\infty} X_{sat}(f)^{\circledast(2k_1-1)} X_{sat}(f)^{\circledast(2k_2-1)} df \right] \quad \text{(B42)}$$

And,

$$\int_{-\infty}^{\infty} Y^2(f)df = \sum_{k_1=1}^{K} \sum_{k_2=1}^{K} c_{2k_1-1}c_{2k_2-1} S^{2(k_1+k_2-1)} = \sum_{k_1=1}^{K} c_{2k_1-1} S^{2k_1-1} \sum_{k_2=1}^{K} c_{2k_2-1} S^{2k_2-1} = \left(\sum_{k=1}^{K} c_{2k-1} S^{2k-1} \right)^2 \quad \text{(B43)}$$

At saturation, $S = 1$ and equation (B43) because of equation (B36) becomes

$$\int_{-\infty}^{\infty} Y^2(f)df = 1 \quad \text{(B44)}$$

Furthermore, the integral of $Y^2(f)$ between two finite frequencies f_a and f_b is

$$\int_{f_a}^{f_b} Y^2(f)df = \sum_{k_1=1}^{K} \sum_{k_2=1}^{k} c_{2k_1-1} \times c_{2k_2-1} S^{2(k_1+k_2-1)} T_{k_1,k_2} \quad \text{(B45)}$$

where

$$T_{k_1,k_2} = \frac{\int_{f_a}^{f_b} X_{sat}^{\circledast(2k_1-1)} X_{sat}^{\circledast(2k_2-1)} df}{\int_{-\infty}^{\infty} X_{sat}^{\circledast(2k_1-1)} X_{sat}^{\circledast(2k_2-1)} df} \quad \text{(B46)}$$

Equation (B46) expresses the interesting result that the entire nonlinear problem is reduced to an algebraic relationship in terms of its characteristics at the saturation point. This allows a great simplification in computer coding and a savings in computer time.

Appendix C

Evaluation of the Multiple Sums Occurring in the Output Spectral Density Function

The first step in the evaluation of the multiple sums occurring in equations (B31) to (B34) is to simplify the notation to

$$X(f)^{\circledast 3} = \sum_{n_1=-N}^{N}{}' \sum_{n_2=-N}^{N}{}' \sum_{n_3=-N}^{N}{}' F(f_{n_1}+f_{n_2}+f_{n_3}) \tag{C1}$$

$$X(f)^{\circledast 5} = \sum_{n_1=-N}^{N}{}' \cdots \sum_{n_5=-N}^{N}{}' F(f_{n_1}+\cdots+f_{n_5}) \tag{C2}$$

$$\vdots$$

$$X(f)^{\circledast K} = \sum_{n_1=-N}^{N}{}' \cdots \sum_{n_k=-N}^{N}{}' F(f_{n_1}+\cdots+f_{n_k}) \tag{C3}$$

Note that equation (C1) can be written as sums over positive integers alone. Thus, the sum over n_3 becomes

$$X(f)^{\circledast 3} = \sum_{n_1=-N}^{N}{}' \sum_{n_2=-N}^{N}{}' \sum_{n_3=1}^{N}{}' \left[F(f_{n_1}+f_{n_2}+f_{n_3})+F(f_{n_1}+f_{n_2}+f_{n_3})\right] \tag{C4}$$

Resolving the sums over n_1 and n_2 in the same way yields

$$\begin{aligned} X(f)^{\circledast 3} = \sum_{n_1=1}^{N}{}' \sum_{n_2=1}^{N}{}' \sum_{n_3=1}^{N}{}' & \left[F(f_{n_1}+f_{n_2}+f_{n_3})+F(-f_{n_1}+f_{n_2}+f_{n_3})\right. \\ & +F(f_{n_1}-f_{n_2}+f_{n_3})+F(-f_{n_1}-f_{n_2}+f_{n_3}) \\ & +F(f_{n_1}+f_{n_2}-f_{n_3})+F(-f_{n_1}+f_{n_2}-f_{n_3}) \\ & \left.+F(f_{n_1}-f_{n_2}-f_{n_3})+F(-f_{n_1}-f_{n_2}-f_{n_3})\right] \end{aligned} \tag{C5}$$

Because n_1, n_2, n_3 are dummy indices whose only purpose is to provide distinctness, they can be interchanged at will. Hence, equation (C5) contains only two combinations of frequencies:

$$\left.\begin{aligned} f_1 &= \pm(f_{n_1}+f_{n_2}+f_{n_1}) \\ f_2 &= \pm(f_{n_1}+f_{n_2}+f_{n_3}) \end{aligned}\right\} \tag{C6}$$

Defining

$$\left.\begin{aligned} H(f_1) &= F(f_1)+F(-f_1) \\ H(f_2) &= F(f_2)+F(-f_2) \end{aligned}\right\} \tag{C7}$$

Equation (C5) can be simplified to

$$X(f)^{\circledast 3} = \sum_{n_1=1}^{N} \sum_{n_2=1}^{N} \sum_{n_3=1}^{N} \left[H(f_{n_1}+f_{n_2}+f_{n_3})+3H(f_{n_1}+f_{n_2}-f_{n_3})\right] \tag{C8}$$

The coefficient 3 in the last term arises from counting the number of ways one negative sign can be distributed over the three frequencies given that permutations of the two positive signs are not distinct; that is,

$$3 = \frac{3!}{1!2!} \tag{C9}$$

Actually the coefficient of the first arises in the same way

$$1 = \frac{3!}{0!3!} \tag{C10}$$

That is, it is the number of ways to distribute zero negative signs over the three frequencies divided by the indistinct number of permutations of the positive sign.

In the case of the fifth-order sums, the same procedure can be applied and gives the following result:

$$\begin{aligned} X(f)^{\circledast 5} = \sum_{n_1=1}^{N} \sum_{n_5=1}^{N} \frac{5!}{0!5!} & \left[H(f_{n_1}+f_{n_2}+f_{n_3}+f_{n_4}+f_{n_5})\right. \\ & + \frac{5!}{1!4!} H(f_{n_1}+f_{n_2}+f_{n_3}+f_{n_4}-f_{n_5}) \\ & \left.+ \frac{5!}{2!3!} H(f_{n_1}+f_{n_2}+f_{n_3}-f_{n_4}-f_{n_5})\right] \end{aligned} \tag{C11}$$

It is clear from these two cases how the higher order sums can be rearranged.

The purpose of this exercise is to reduce the number of calculations that must be made. The total number of frequency computations in equations (C1) and (C2) is $(2N)^3$ and $(2N)^5$. Of these, most are redundant. The rearrangements given in equations (C8) and (C11) reduce these to $2N^3$ and $3N^5$ a factor of 1/4 and 3/32, respectively. For the seventh-order sums, the reduction factor is 1/32; and for the ninth order, only 5/128 of the total calculations are required. However, the remaining calculations are still many and further reductions are needed. These can be made through the narrow band approximation which reduces the calculations from $(2N)^K$ to N^K.

Let

$$f = f_0 + \nu \tag{C12}$$

where

$$-W \leq \nu \leq W \tag{C13}$$

where $2W$ is the bandwidth. In the narrow band approximation the computations are limited to the band of frequencies centered on f_0. Therefore, the first term in equation (C8) can be ignored because its argument is centered on $3f_0$. Likewise, the first and second terms of the fifth-order convolution in equation (C11) can be ignored because they are centered on $5f_0$ and $3f_0$. For each of the convolutions the terms that are retained have the following arguments:

Third order: $f_{n_1} + f_{n_2} - f_{n_3}$

Fifth order: $f_{n_1} + f_{n_2} + f_{n_3} - f_{n_4} - f_{n_1}$

Seventh order: $f_{n_1} + f_{n_2} + f_{n_3} + f_{n_4} - f_{n_5} - f_{n_6} - f_{n_7}$ (C14)

etc.

In order to compute the resultant frequencies given in equation (C14), we let

$$f_{n_i} = f_0 + k_{n_i} w \tag{C15}$$

where w is an appropriate increment and k_{n_i} is an integer. Such a conversion of frequencies to integers can always be accomplished with arbitrary accuracy. The third-order frequencies (from eq. (C14)) can then be written

$$f_{n_1} + f_{n_2} - f_{n_3} = f_0 + (k_{n_1} + k_{n_2} - k_{n_3}) w \tag{C16}$$

Obviously, the combination of integers $(k_{n_1} + k_{n_2} - k_{n_3})$ is also an integer. The same is true for orders higher than third.

If the structure of input frequencies is complicated and/or the order of intermodulation products is high, it is convenient to use a computer to calculate the frequencies in equation (C14). A computer program has been written in which the various orders are computed recursively. The program coding will not be given here, but its computational procedures will be outlined.

First, a second-order set of integers is computed; namely,

$$K_i^{(2)} = k_{n_1} - k_{n_2} \quad \begin{cases} n_1 = 1, \ldots, N \\ n_2 = 1, \ldots, N \end{cases} \tag{C17}$$

Associated with these numbers is an amplitude factor given by

$$A_i^{(2)} = a_{n_1} a_{n_2} \tag{C18}$$

The range of i in both of these equations is clearly between 1 and N_2.

The third-order set of integers and the associated amplitude factor can now be computed

$$\left.\begin{aligned} K_{m'}^{(3)} &= k_{n_1} + K_i^{(2)} \\ A_{m'}^{(3)} &= a_{n_1} A_i^{(2)} \end{aligned}\right\} \quad \begin{aligned} n_1 &= 1, \ldots, N \\ i &= 1, \ldots, N^2 \end{aligned} \tag{C19}$$

If the calculations in equation (C19) were carried out as indicated, then there would be N^3 integers and amplitude factors. However, not all of the $K_{m'}^{(3)}$ integers are unique. For each redundancy the amplitude factors are added and become a weighting function. Hence,

$$\begin{aligned} K_m^{(3)} &= k_{n_1} + K_i^{(2)} \\ A_m^{(3)} &= \sum_{m'} A_{m'}^{(3)} \end{aligned} \tag{C20}$$

The range of m is from 1 to $N^{(3)}$ in which $N^{(3)}$ is considerably less than N^3.

The fifth-order terms are now computed from

$$\left.\begin{aligned} K_m^{(5)} &= K_i^{(2)} + K_j^{(3)} \\ A_m^{(5)} &= \sum_m A_i^{(2)} A_j^{(3)} \end{aligned}\right\} \quad \begin{aligned} &i = 1, \ldots, N^2 \\ &j = 1, \ldots, N^{(3)} \end{aligned} \tag{C21}$$

where

$$m = 1, \ldots, N^{(5)} << N^5$$

Again, in the computations of equation (C21) the accounting for redundancy is indicated by the sum over m and results in $N^{(5)}$ values.

The seventh-order terms are

$$\left.\begin{aligned} K_m^{(7)} &= K_i^{(2)} + K_j^{(5)} \\ A_m^{(7)} &= \sum_m A_i^{(2)} A_j^{(5)} \end{aligned}\right\} \quad \begin{aligned} &i = 1, \ldots, N^2 \\ &j = 1, \ldots, N^{(5)} \end{aligned} \tag{C22}$$

where

$$m = 1, \ldots, N^{(7)} << N^7$$

And, finally, the ninth-order terms are

$$\left.\begin{aligned} K_m^{(9)} &= K_i^{(2)} + K_j^{(7)} \\ A_m^{(9)} &= \sum_m A_i^{(2)} A_j^{(7)} \end{aligned}\right\} \quad \begin{aligned} &i = 1, \ldots, N^2 \\ &j = 1, \ldots, N^{(7)} \end{aligned} \tag{C23}$$

where

$$m = 1, \ldots, N^{(9)} << N^9$$

The program is limited to the ninth order but it can be easily extended to higher orders.

The purpose of these calculations is to compute the amount of signal distortion that is introduced by the nonlinearity. But not all of the nonlinear terms in equation (B4) can be considered as noise. The higher terms do contribute to a coherent amplification of the input signal. If we assume that the information will be carried on the amplitude factors, then crosstalk and other distortions can be attributed to terms involving cross products of amplitudes. Therefore, using equations (B30) to (B34), (C12), (C14), and (C15) and considering only the positive frequencies result in the coherent terms being

$$X_c(f) = \sum_{n=1}^{N} a_n e^{-\lambda(\nu - k_n w)^2} \tag{C24}$$

$$X_c(f)^{\circledast 3} = \frac{1}{\sqrt{3}} \left(\frac{\pi}{\lambda}\right) \sum_{n=1}^{N} a_n^3 e^{-(\lambda/3)(\nu - k_n w)^2} \tag{C25}$$

$$X_c(f)^{\circledast 5} = \frac{1}{\sqrt{5}} \left(\frac{\pi}{\lambda}\right)^2 \sum_{n=1}^{N} a_n^5 e^{-(\lambda/5)(\nu - k_n w)^2} \tag{C26}$$

$$X_c(f)^{\circledast 7} = \frac{1}{\sqrt{7}} \left(\frac{\pi}{\lambda}\right)^3 \sum_{n=1}^{N} a_n^7 e^{-(\lambda/7)(\nu - k_n w)^2} \tag{C27}$$

$$X_c(f)^{\circledast 9} = \frac{1}{\sqrt{9}} \left(\frac{\pi}{\lambda}\right)^4 \sum_{n=1}^{N} a_n^9 e^{-(\lambda/9)(\nu - k_n w)^2} \tag{C28}$$

And the general term where K is an integer is

$$X_c(f)^{\circledast(2K+1)} = \frac{1}{\sqrt{2K+1}} \left(\frac{\pi}{\lambda}\right)^K \times \sum_{n=1}^{N} a_n^{(2K+1)} e^{-\lambda(\nu - k_n w)^2/(2K+1)} \tag{C29}$$

Finally, the complete expressions for the convolutions including the coherent terms are as follows:

$$X(f)^{\circledast 3} = \frac{1}{\sqrt{3}} \left(\frac{\pi}{\lambda}\right) \sum_{m=1}^{N^{(3)}} A_m^{(3)} e^{-\lambda(\nu - K_m^{(3)} w)^2/3} \tag{C30}$$

$$X(f)^{\circledast 5} = \frac{1}{\sqrt{5}} \left(\frac{\pi}{\lambda}\right)^2 \sum_{m=1}^{N^{(5)}} A_m^{(5)} e^{-\lambda(\nu - K_m^{(5)} w)^2/5} \tag{C31}$$

$$X(f)^{\circledast 7} = \frac{1}{\sqrt{7}}\left(\frac{\pi}{\lambda}\right)^{3} \sum_{m=1}^{N^{(7)}} A_m^{(7)} e^{-\lambda(\nu - K_m^{(7)} w)^2/7} \qquad \text{(C32)}$$

$$X(f)^{\circledast 9} = \frac{1}{\sqrt{9}}\left(\frac{\pi}{\lambda}\right)^{4} \sum_{m=1}^{N^{(9)}} A_m^{(9)} e^{-\lambda(\nu - K_m^{(9)} w)^2/9} \qquad \text{(C33)}$$

And the general Kth term is

$$X(f)^{\circledast(2K+1)} = \frac{1}{\sqrt{2K+1}}\left(\frac{\pi}{\lambda}\right)^{K} \times \sum_{m=1}^{N^{(K+1)}} A_m^{(2K+1)} e^{-\lambda[\nu - K_m^{(2K+1)} w)]^2/(2K+1)} \qquad \text{(C34)}$$

1. Report No.	2. Government Accession No.	3. Recipient's Catalog No.
NASA TP-1999		

4. Title and Subtitle	5. Report Date
COMPUTER MODELING OF MULTIPLE-CHANNEL INPUT SIGNALS AND INTERMODULATION LOSSES CAUSED BY NONLINEAR TRAVELING-WAVE-TUBE AMPLIFIERS	May 1982
	6. Performing Organization Code 541-02-12

7. Author(s)	8. Performing Organization Report No.
N. Stankiewicz	E-722
	10. Work Unit No.

9. Performing Organization Name and Address	11. Contract or Grant No.
National Aeronautics and Space Administration Lewis Research Center Cleveland, Ohio 44135	

12. Sponsoring Agency Name and Address	13. Type of Report and Period Covered
National Aeronautics and Space Administration Washington, D.C. 20546	Technical Paper
	14. Sponsoring Agency Code

15. Supplementary Notes

16. Abstract

The multiple-channel input signal to a soft limiter amplifier such as a traveling wave tube is represented as a finite, linear sum of Gaussian functions in the frequency domain. Linear regression is used to fit the channel shapes to a least-squares residual error. Distortions in output signal, namely intermodulation products, are produced by the nonlinear gain characteristic of the amplifier and constitute the principal noise analyzed in this study. The signal-to-noise ratios are calculated for various input powers from saturation to 10 dB below saturation for two specific distributions of channels. A criterion for the truncation of the series expansion of the nonlinear transfer characteristic is given. It is found that the signal-to-noise ratios are very sensitive to the coefficients used in this expansion. Improper or incorrect truncation of the series leads to ambiguous results in the signal-to-noise ratios.

17. Key Words (Suggested by Author(s))	18. Distribution Statement
Intermodulation products TWT nonlinearities Signal distortions	Unclassified - unlimited STAR Category 33

19. Security Classif. (of this report)	20. Security Classif. (of this page)	21. No. of Pages	22. Price*
Unclassified	Unclassified	24	A02

* For sale by the National Technical Information Service, Springfield, Virginia 22161

NASA-Langley, 1982

National Aeronautics and
Space Administration

Washington, D.C.
20546

Official Business
Penalty for Private Use, $300

THIRD-CLASS BULK RATE

Postage and Fees Paid
National Aeronautics and
Space Administration
NASA-451

U.S.MAIL

2 1 U.,J. 820524 S00903DS
DEPT OF THE AIR FORCE
AF WEAPONS LABORATORY
ATTN: TECHNICAL LIBRARY (SUL)
KIRTLAND AFB NM 87117

NASA

POSTMASTER: If Undeliverable (Section 158 Postal Manual) Do Not Return